# Single-Molecule Adhesion of a Stimuli-Responsive Oligo(ethylene glycol) Copolymer to Gold

Michael A. Nash* and Hermann E. Gaub

Lehrstuhl für Angewandte Physik and Center for NanoScience, Ludwig-Maximilians-Universität, 80799 Munich, Germany

ABSTRACT Adhesion of environmentally responsive polymers to biocompatible surfaces is an important issue that has been explored in several nanobiotechnology applications. Here, we prepared multi-responsive statistical copolymers of two oligo(ethylene glycol) methyl ether methacrylate macromonomers with differing ethylene glycol side chain lengths using RAFT polymerization. The lower critical solution temperature of the copolymers was characterized using visible light extinction, and the chemical composition and

molecular weight were measured using NMR spectroscopy and size-exclusion chromatography, respectively. The characterization results demonstrated that the transition temperature could be controlled by varying the macromonomer feed ratios, and the molecular weight could be controlled by varying the amount of the RAFT chain transfer agent in the polymerization feed. Using AFM single-molecule force spectroscopy, we measured the adhesion characteristics of single copolymer molecules to a gold surface. We found that dehydration and collapse of the copolymer in a high ionic strength buffer resulted in dramatically reduced bridging length distributions that maintained their single-molecule bimodal character. In the collapsed state, the polymer exhibited a lower absolute desorption force while cooperativity effects were found to increase the desorption force per chain for multi-chain interactions. Our results confirmed that the polymer in a collapsed conformation exhibited a dramatically reduced volume occupancy above the gold surface. These results demonstrate at the single-molecule level how solvent-induced collapse of an environmentally responsive copolymer modulates surface adhesion forces and bridging length distributions in a controllable way.
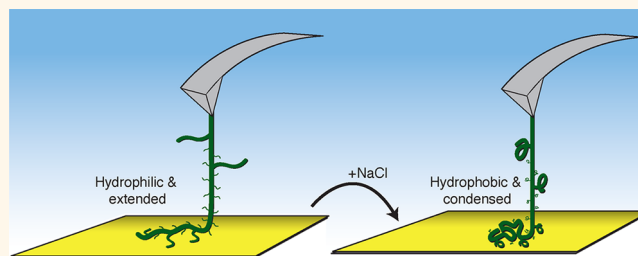
KEYWORDS: single-molecule force spectroscopy · RAFT polymer · oligo(ethylene glycol) methyl ether methacrylate

Intelligent materials that sense and respond to environmental stimuli actively undergo changes in structural properties to provide an output signal. Smart polymeric materials are being developed which couple these changes with the control of molecular activity, such as adhesion to surfaces. Polymer adhesion to inorganic biocompatible materials is fundamentally important in many biotechnology applications, including treatment of medical device surfaces,[1] functionalization of biosensors,[2] and modification of inorganic nanoparticles for drug delivery.[3] In such systems, local environmental effects related to polymer composition and macromolecular conformation determine how polymers interact with surfaces and biological media.

Measurement of smart polymer adhesion has been achieved using various methods, including quartz crystal microbalance,[4] fluorescence assays,[5] and surface plasmon resonance.[6] An alternative method, molecular force spectroscopy, is a biophysical method for measuring the response of macromolecules to external forces. This single-molecule method has been used to measure synthetic polymer surface adhesion,[7,8] providing adhesion parameters such as the adhesion free energy per monomer unit, as well as kinetic binding coefficients between the polymer and cosolutes.[9]

Poly(ethylene glycol) (PEG) is a hydrophilic polymer widely used in industrial and biomedical settings. PEG-functionalized surfaces exhibit low nonspecific binding when contacted with blood,[10] a property that has been used to passivate biomedical diagnostic device surfaces for decades. Linear PEG, however, is not easily polymerized in block or branched architectures, and end group
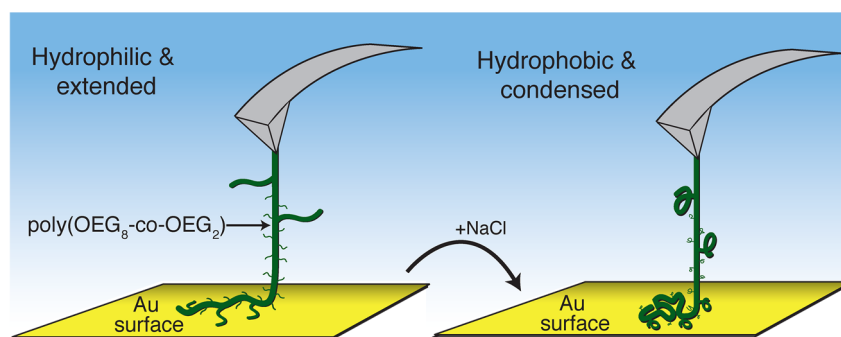
Figure 1. In response to an increase in NaCl, a poly(oligo ethylene glycol) copolymer reversibly transitions from an expanded hydrated conformation (left) to a condensed hydrophobic globule (right). This conformational change alters adhesion characteristics such as desorption force and bridging length.

modification can be involved. Recently, new nano/bio research areas have emerged (*e.g.*, separations, targeted drug delivery, controlled release, biomaterials) requiring active and biocompatible surfaces that are able to respond to external stimuli and carry out biomolecular action. Within this context, polymers composed of oligo(ethylene glycol) methyl ether methacrylates (OEG-MA) have proven extremely versatile in terms of synthetic flexibility and biochemical properties.[11−13]

OEG-MA polymers comprise a carbon−carbon backbone with comb-like OEG side chains of variable length. Poly(OEG-MA) polymers can be synthesized from OEG macromonomers using a variety of controlled free-radical polymerization methods, including ATRP[14] and RAFT.[15] The resulting OEG-MA copolymers are more hydrophobic than linear PEG, but because they consist of 85% ethylene glycol residues by weight, they are also biocompatible and water-soluble. Moreover, OEG-MA polymers are thermally responsive and undergo a hydrophilic to hydrophobic phase transition in response to environmental stimuli (*e.g.*, salt, temperature). The transition temperature of OEG-MA polymers can be tuned over a wide range from 0 to 100 °C by varying the side chain lengths and ratios of the OEG-MA macromonomers.[16] The transition temperature can also be made pH-dependent by copolymerizing monomers with titratable groups (*e.g.*, amine, carboxyl). The resulting OEG-MA block polyelectrolytes can be made responsive to pH, temperature, and salt.[17] Despite the known complementary features of RAFT polymerization and OEG-MA polymers for providing tunable and responsive materials, these features have never been combined or exploited for AFM-based adhesion studies.

Single-molecule adhesion measurements using AFM force spectroscopy provide information about synthetic and biopolymer adhesion to inorganic surfaces. Typically, polymer molecules are conjugated to a silicon microcantilever tip that is contacted with an inorganic surface. As the cantilever is retracted, a single or a few polymer molecules bridge the distance between the tip and surface, imposing a downward force on the cantilever that can be measured using the optical lever technique (Figure 1). The adhesion force experienced by the cantilever is governed by an interplay of entropic and enthalpic contributions of the adsorbed polymer. Plateaus in the force *versus* distance trace are known to occur when the binding and rebinding of polymer segments with the surface occur much faster than the experimental sampling rate. The desorption force represents the adhesion free enthalpy per unit length, and if this energy is constant, the force exhibits a plateau. This will typically occur when the polymer is weakly adsorbed and mobile on the surface, allowing for peeling or sliding of the polymer during the pull-off process.[7,18] The measured distribution of desorption pleateau forces characterizes the strength of the adhesion, while the bridging lengths can be used to characterize the contour length of individual polymer molecules.[19] Quantized plateaus of constant force such as those shown here are also observed in the unzipping of DNA duplexes[20] and unfolding of fibrous amyloid proteins.[21]

RESULTS AND DISCUSSION

We prepared an environmentally responsive statistical copolymer of two oligo(ethylene glycol) methyl ether methacrylate (OEG$_n$-MA) macromonomers with variable OEG side chain lengths of 2 or 8.5 ethylene glycol repeat units, as shown in Figure 2A. The RAFT chain transfer agent used during the polymerization step afforded polymers with semi-telechelic functional groups comprising a carboxyl group at the α end and a −C$_{12}$H$_{25}$ hydrocarbon tail at the ω end. The molecular weight of the polymer was ∼220 kDa for the sample used in this study. Size-exclusion chromatograms can be found in Supporting Figure 1, and the ^{1}H NMR spectrum is shown in Supporting Figure 2.

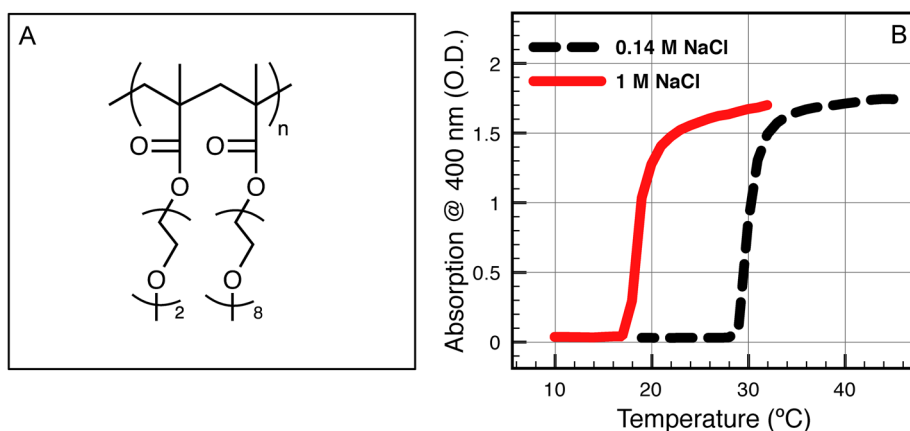The lower critical solution temperature (transition temperature) of the copolymer was measured using

Figure 2. Poly(oligo(ethylene glycol) methyl ether methacrylate) copolymer was prepared using RAFT polymerization. Dependent upon the OEG$_2$ to OEG$_8$ ratio, the phase transition point could be set near room temperature in response to temperature and salt stimuli. (A) Chemical structure of the polymer. (B) Cloud-point curves (cooling) measured in 0.14 and 1 M NaCl/phosphate buffer, pH 7.4.

visible light absorption (cloud-point) measurements, shown in Figure 2B. The polymer was dissolved at 2 mg/mL in phosphate buffered saline (PBS, pH 7.4) containing 0.14 or 1 M NaCl. The turbidity was then monitored at 400 nm as the sample temperature was varied over a range between 10 and 45 °C at a rate of 0.2 °C/min. A rapid increase above ∼30 °C for the sample dissolved in 0.14 M NaCl was characteristic of the polymer phase transition. In the higher salt PBS buffer containing 1 M NaCl, the transition temperature was shifted downward below 20 °C, attributable to the Hofmeister effect.[22] A mass loading ratio of 20% OEG$_8$-MA to 80% OEG$_2$-MA in the polymerization feed was found to produce polymers with the desired phase transition temperature around 30 °C in standard 0.14 M NaCl/PBS buffer. Increasing the amount of OEG$_8$-MA in the polymerization feed tended to increase the phase transition temperature due to the increased hydrophilicity of the OEG$_8$-MA monomer as compared with OEG$_2$-MA, consistent with previously published observations.[12] Cloud-point traces for polymers containing variable amounts of OEG$_8$-MA (30 and 10%) can be found in Supporting Figure 3. The polymer's phase transition could also be triggered under isothermal conditions at room temperature upon addition of NaCl, which was the preferred method for further AFM studies.

Details regarding the surface and cantilever preparation can be found in the Supporting Information. A V-shaped silicon nitride cantilever (MLCT-C lever, Bruker) with a low nominal spring constant of ∼10 pN/nm was modified with 3-aminopropyl-dimethylethoxysilane, according to previously published procedures.[20] The RAFT chain transfer agent provided the resulting linear copolymers with a carboxyl group at the α end, which was used in conjunction with carbodiimide coupling to attach the polymers to the AFM cantilever. The ω end of the RAFT

agent ($-C_{12}H_{25}$) was presented toward the gold surface during AFM desorption experiments. Evaporated gold surfaces were cleaned with ammonia and hydrogen peroxide (RCA cleaning) and rinsed thoroughly with purified water prior to use. Control experiments with bare tips prior to the covalent functionalization showed in rare cases short-ranged attractive interactions which might be attributed to contaminations, but no desorption traces with the well-pronounced plateaus as they are described in the experiments were found.

AFM measurements were performed on an instrument designed and built in-house running on custom-written IGOR PRO software in conjunction with an MFP-3D AFM controller (Asylum Research). Calibration of the polymer-modified cantilever in standard PBS buffer containing 0.14 M NaCl was performed using the equipartition theorem, resulting in a spring constant of 14.72 pN/nm. The AFM was automated to acquire force−extension traces at z-piezo retraction velocities of 500, 1500, and 5000 nm/s. All AFM measurements were made at 22 °C. The data sampling rate was set to 5e3, 10e3, and 20e3 Hz for the retraction velocities of 500, 1500, and 5000 nm/s, respectively. A low-pass filter at one-half the sampling rate was used in all cases.

As shown in Figure 3A, force−extension traces of the OEG-MA copolymer in PBS (0.14 M NaCl) on an un-modified polycrystalline gold surface exhibited quantized plateaus of constant force that decreased in discrete steps downward. Such stepwise character observed in the force−extension traces is known to occur when a polymer interacts with a surface in equilibrium desorption mode, where it is adsorbed yet mobile on the surface.[7,9,18,23,24] Each step in the force−extension trace corresponded to a desorption event of a single or a few polymer chains from the surface. The maximal distance from the surface at which a step was observed before the force dropped
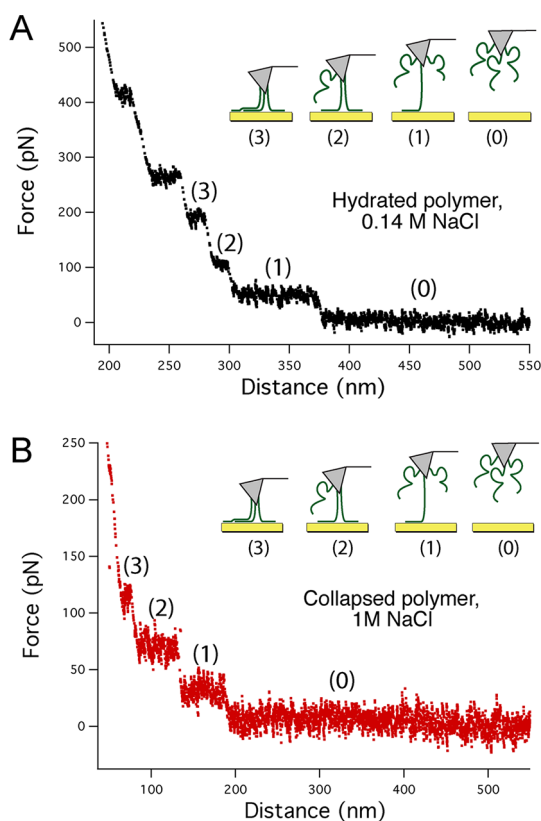
Figure 3. Single polymer molecule desorption. A polymer-modified AFM cantilever was contacted with a bare gold surface and retracted at 500 nm/s while measuring the adhesion force on the cantilever. Polymer molecules in both an expanded/hydrated (A, black) and a collapsed/dehydrated conformation (B, red) exhibited force plateaus characteristic of equilibrium desorption mode.

Figure 4. Histograms of polymer bridging lengths. Force—distance traces from the same cantilever in two solvents (0.14 M NaCl (black) and 1 M NaCl (red)) were searched for desorption steps using automated computer analysis. Histograms of the distance at which the last polymer molecule desorbed (last rupture distance) showed pronounced bimodal distributions. Collapse of the polymer upon addition of NaCl dramatically shortened the rupture distances and maintained the bimodal distribution.

to 0 pN is referred to as the "bridging length". In Figure 3A, a bridging length of approximately 375 nm can be seen. After acquiring several thousand force—extension traces, such as those shown in Figure 3A, over the course of several hours, the solvent was changed to PBS containing 1 M NaCl, and the cantilever was recalibrated using the equipartition theorem, yielding a value of 12.37 pN/nm. At the high NaCl concentration, the polymer was expected to be in a condensed hydrophobic conformation, in accordance with the cloud-point measurements of Figure 2B. As shown in Figure 3B, force—extension traces obtained with the same cantilever also exhibited plateaus of constant force in the PBS containing 1 M NaCl that decreased stepwise downward, indicating that in the high salt buffer the polymer interacted with the surface in equilibrium desorption mode, as well.

An automated computer analysis routine was implemented to determine the bridging length distributions for the polymer in each solvent, the results from which are shown in Figure 4. In PBS containing 0.14 M NaCl, the distribution of bridging lengths was bimodal with one population centered at 370 nm
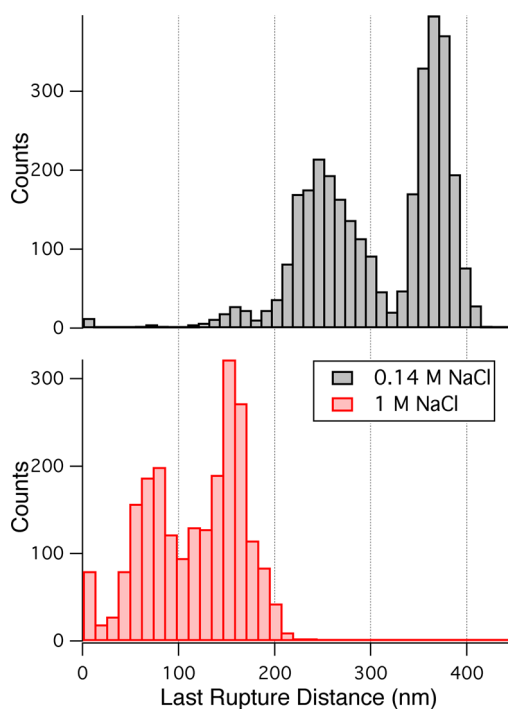
and another slightly broader population centered around 250 nm (Figure 4, top, black). The bimodal distribution was attributed to the presence of two polymer molecules of differing contour length on the cantilever interacting with the gold surface. Upon polymer phase separation in the high salt (1 M NaCl) PBS buffer, the bimodal distribution was maintained, but the bridging lengths were dramatically reduced, as shown in Figure 4 (bottom, red). The bimodal peaks in the high salt buffer were centered at 160 and 70 nm.

The condensed/collapsed conformation of the polymer in the high salt buffer resulted in an entropic penalty imposed on the system as the polymer bridged the surface and cantilever. As the polymer was extended away from the surface, an increase in the hydrophobic polymer's contact area with water imposed an energetic limit, reducing the achievable bridging lengths. The results can be interpreted in the context of a competitive adhesion model that has been previously postulated.[19] The gold surface and the polymer-coated cantilever tip compete for adsorption of the bridging polymer. Since the AFM tip was modified with multiple environmentally responsive polymer chains, in the high salt buffer, we can speculate the polymers on
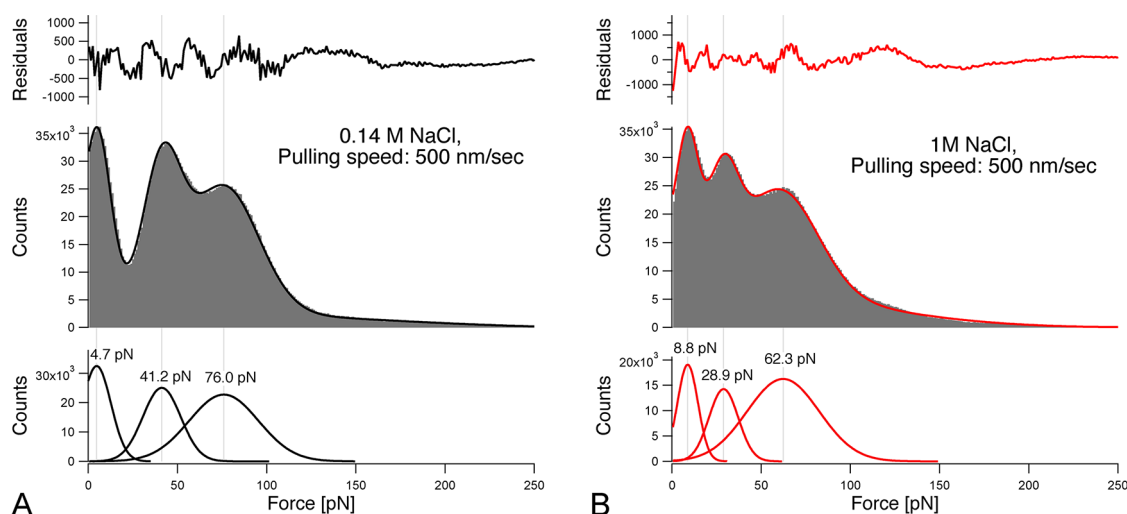
Figure 5. Histograms of desorption forces. Portions from force—distance traces corresponding to the last two desorption events were selected. Histograms of the measured forces showed trimodal distributions with peaks corresponding to desorption plateau step heights. The first peak at low force was attributed to viscous drag on the cantilever and represents the force measurement background. Gaussian fits (bottom panels) of the histograms provided the desorption forces of individual polymer chains, which were larger in hydrated (A, left) *vs* condensed (B, right) states. The overall multi-Gaussian fits to the observed force distributions are shown in the middle panels (A, solid black line; B, solid red line).

the tip could out compete the Au surface for the bridging polymer binding sites at a shorter distance away from the surface, as compared with the low salt case.

Prior measurements on elastin-like polypeptides and poly(*N*-isopropylacrylamide), two well-known environmentally responsive polymers with analogous phase separation properties, have shown decreased polymer volume occupancy in high salt aqueous buffers[25,26] or above the transition temperature[27] when probed with AFM. These results were supported by the notion that a loss of "caged" or clathrate-like water molecules resulted in phase transition to a condensed state, with a corresponding decrease in physical dimensions, where the polymer adopted an increasingly collapsed conformation with increasing salt. In the prior studies, however, equilibrium desorption behavior was never probed, and single molecules adhering to the surface were not resolved. The condensed conformation of the polymers in the prior work was indirectly inferred *via* an altered indentation curve in the high salt buffer, which showed an increase in the Young's modulus of the surface. Unlike these prior works, we were able to measure the change in volume occupancy and adhesion characteristics of the single polymer molecules directly because of the equilibrium desorption mode of binding that this particular polymer formulation exhibited on the polycrystalline gold surface.

In rare cases (~2%), the force—extension traces exhibited a nonlinear entropic spring-type behavior instead of plateaus of constant force. This was attributed to coordination bonding between the trithiocarbonate

polymer end group and the gold surface, resulting in polymer pinning and loss of polymer mobility on the surface. Trithiocarbonates are known to bind gold surfaces with densities similar to self-assembled thiol monolayers.[28] To analyze traces where pinning of the polymer end group occurred, we used a worm-like chain (WLC) model[29] to estimate the persistence length of the polymer in each of the two buffers. Two exemplary data traces with WLC models are shown in Supporting Figures 4 and 5, and a comparison of all persistence length fits is shown in Supporting Figure 6. These data suggest that the polymer persistence length may be slightly lower in the high salt buffer. Whether or not this is a real effect or a limitation of the model remains open for debate. The WLC model assumes non-interacting chains, and for our polymers in the hydrophobic state, this may not be appropriate.

In addition to a shortened bridging length distribution, analysis of force—extension traces also yielded information about differences in equilibrium desorption forces between the hydrophilic/extended and hydrophobic/collapsed polymers adsorbed to the gold substrate. For the analysis of absolute desorption forces, a range of distance values was selected in each solvent, corresponding to the distance at which the last few polymer molecules desorbed (*i.e.*, the last few steps of the force—extension traces). For example, for the sample in 0.14 M NaCl, the force values between 250 and 400 nm were assembled into a histogram and fitted with Gaussian distributions to estimate the equilibrium desorption force. For the same cantilever in 1 M NaCl, the force values within a range of 50 and 175 nm away from the surface were

histogrammed. There was no preselection of curves, so all of the 2303 in curves obtained in 1 M NaCl and the 3249 obtained in 0.14 M NaCl were used to assemble the histograms. The results from such an analysis are shown in Figure 5.

In Figure 5A (middle), the number of data points obtained at a given force value are plotted *versus* the measured force. Three peaks are clearly visible, fitted with Gaussian distributions (bottom). In Figure 5A (top), the residuals from the Gaussian fit are shown. Peaks corresponding to 0, 1, and 2 polymer molecules adsorbed to the gold surface are observed in the force histograms. The peak at low force yielded a Gaussian fit with a mean of 4.7 pN. This background force value is measured due to a viscous drag on the cantilever close to the surface.[30] The difference in the dynamic viscosity between the 0.14 M NaCl and 1 M NaCl buffers is 88 μPa·s, or an 8.8% increase when switching to the 1 M NaCl buffer.[31] Since the AFM data import routine averaged the last 10% of the force trace and offset the force values such that 0 pN was reached at the end of each trace, the absolute viscosity difference between the two solvents does not play a role in the assembled histograms. The increase in the background force from 4.7 pN in the 0.14 M NaCl solvent to 8.8 pN in the 1 M NaCl solution was observed because the histogram in 1 M NaCl was assembled from force measurements acquired closer to the surface.

In addition to the background force peaks, peaks corresponding to one and two polymer molecules adsorbed to the gold surface were observed in the force histograms. In the 0.14 M NaCl/PBS, single-molecule desorption forces with a mean of 41.2 pN were measured. After subtracting the background level of 4.7 pN from this value, a mean desorption force of 36.5 pN is obtained, corresponding to a desorption free energy of 8.96 k_BT/nm for the single molecule. For the peak corresponding to two molecules, a value of 76.0 pN was obtained. After subtracting the background value, a desorption force of 71.3 pN or desorption free energy of 17.5 k_BT/nm was obtained. From this analysis, we see that the adsorption free energy of two molecules is approximately 2 times the adsorption free energy of the single-molecule events ($\pm$4.6%), suggesting that the measured force in the low salt buffer is a combination of two independent adsorption forces, and that the polymers do not strongly interact with each other.

Using the same analysis method for the data set obtained from the same cantilever in 1 M NaCl/PBS, after subtracting the background peak from the fitted Gaussian distributions of the force histograms, a single-molecule desorption force of 20.1 pN or desorption free energy of 4.93 k_BT/nm was obtained, as shown in Figure 5B. Comparing the single-molecule desorption plateaus between the two solvents, we see that the adsorption free energy decreased by 45% in the high salt buffer, significantly larger than any expected deviation due to uncertainty in the cantilever spring constant ($\pm$10%).

Two-molecule desorption pleateaus measured at 62.3 pN minus the 8.8 pN background value resulted in a desorption force of 53.5 pN, which corresponds to 13.1 k_BT/nm. In contrast to the sample in 0.14 M NaCl/PBS, the adsorption free energy of two molecules in the high salt buffer was 33% higher than 2 times the single-molecule desorption free energy. The 33% increase in desorption force per molecule for the two-molecule case in the poor solvent could be explained by co-operativity effects. Polymers in the condensed state are known to undergo intermolecular agglomeration in bulk solution, as was observed in the absorbance measurements (Figure 2B). The AFM result is consistent with cooperative polymer—polymer interactions in the high salt buffer increasing adsorption force per mono-mer. The collapsed polymers interact strongly with one another, and the resulting adhesion forces are conse-quently not an integer multiple of the basal adhesion force. In general, the desorption forces were not strongly dependent on the pulling speed, which were varied from 500 to 5000 nm/s. Pulling speed depen-dence of the desorption plateau height can be found in Supporting Figure 7.

CONCLUSION

Here we presented single-molecule measurements of environmentally responsive polymer adhesion in equilibrium desorption mode. Differences in bridging length distributions and adhesion forces were found to be dependent on the conformation of the polymer, which could be switched at room temperature upon addition of salt. The collapsed polymer conformation exhibited a dramatically shortened bridging length distribution (Figure 4), as well as a decrease in absolute adhesion forces (Figure 5). The adhesion force of two molecules was approximately 2 times the single-molecule basal adhesion force in the extended state, where polymer—polymer interactions were expected to be negligible. In the high salt buffer, the single-molecule adhesion force of the collapsed polymer was significantly lower than for the extended polymer in the low salt buffer. The adhesion force of two polymer molecules in the high salt buffer was approximately 33% greater than 2 times the single-molecule adhesion force in the same solvent. The overall decrease in single-molecule adhesion force in the high salt buffer likely explains the dramatic decrease in bridging lengths. Intermolecular polymer—polymer aggrega-tion likely competes with surface adhesion, providing an alternative unbinding pathway. The main findings we report in this paper describing the polymer's quantized bridging length distribution on a gold sur-face are expected to be applicable to other biomaterial

surfaces where the polymer exhibits the same equilibrium mode of binding. In this regard, titanium, another biocompatible metal, would be an interesting candidate for follow up studies.

METHODS

Polymer Synthesis. Poly(ethylene glycol) methacrylate (M_n = 475 g/mol, 100 ppm MEHQ, 200 ppm BHT inhibitor) and di(ethylene glycol) methyl ether methacrylate (M_n = 188.22) were purchased from Sigma and purified through a neutral aluminum oxide column prior to use. The chain transfer agent 4-cyano-4-[(dodecylsulfanylthiocarbonyl)sulfanyl]pentanoic acid (M_n = 403.67) was purchased from Sigma and used as received. The initiator 2,2′-azobis(2-methylpropionitrile) (AIBN, M_n = 164.21) was purchased from Sigma and recrystallized from methanol prior to use. In a typical RAFT polymerization, 0.8 g of the di(ethylene glycol) methyl ether methacrylate and 0.2 g of the poly(ethylene glycol) methacrylate were placed into a round-bottom flask. Next, 0.93 mg of the chain transfer agent and 90 μg of the initiator dissolved in dioxane were added. Dioxane was then added such that the mass ratio of dioxane to monomers was 2:1. The flask was next purged for 30 min with N_2. The reaction proceeded for 17 h at 70 °C and was then precipitated into a 1:1 mixture of hexane/ether at 4 °C. The gummy precipitate was next dissolved into tetrahydrofuran and precipitated two more times into cooled 1:1 ether/hexane mixtures. Finally, the product was collected by centrifugation and dried under vacuum for 3 h. Residual monomers and impurities were removed *via* PD10 desalting column (GE Healthcare) in water or alternatively by dialysis.

Polymer Analysis. Organic size-exclusion chromatography in THF with multi-angle light scattering was performed through contract service with Polymer Standards Service GmbH (Mainz, Germany). The polymer was dissolved at 3.3 or 5.5 mg/mL, and 100 μL was injected at a flow rate of 1 mL/min at 25 °C. Multi-angle light scattering was used for absolute molecular weight determination. For the polymer sample used in the AFM measurements, the targeted M_w was 500 kDa, the dn/dc value obtained was 0.078 mL/g, while the measured M_w = 220 kDa, M_n = 155 kDa, and PDI = 1.4. ^{1}H NMR was performed at 8 mg/mL in CDCl$_3$ on an Avance III 600 MHz NMR spectrometer (Bruker, Karlsruhe).

Conjugation of Polymers to Cantilevers. Silicon nitride AFM cantilevers (MLCT-lever C, nominal spring constant ~10 pN/nm) were purchased from Bruker. Levers were activated by 15 min UV-ozone treatment followed by modification with 3-aminopropyldimethylethoxysilane following previously published procedures (see main text, ref 19). Amino-silanized cantilevers were placed in sodium borate buffer (150 mM, pH 8.5) for 30 min to deprotonate amine groups. Next, the 220 kDa poly(oligo(ethylene glycol)) copolymer was dissolved at 100 mg/mL in sodium phosphate buffer (10 mM phosphate, 137 mM NaCl, pH 7.4). Then, 50 mg/mL of 1-ethyl-3-(3-dimethylaminopropyl)carbodiimide (EDC, Thermo Scientific) and 50 mg/mL of N-hydroxysulfosuccinimide (Sulfo-NHS, Thermo Scientific) were added, and the solution was applied to the deprotonated amino cantilevers. The conjugation to the cantilever proceeded for 1 h at room temperature. Finally, the cantilevers were rinsed in purified water and stored under phosphate buffered saline for several minutes before AFM measurements.

Gold Surface Preparation. Circular glass coverslips 22 mm in diameter were cleaned by sonication in isopropyl alcohol/water (1:1). A 2 nm thick layer of Ni/Cr was evaporated onto the cleaned coverglass, followed by a 30 nm thick Au layer using a thermal evaporator. Prior to AFM measurements, gold surfaces were cleaned using 15 min UV-ozone treatment, followed by 3 min etching in a mixture of H_2O, NH_3 (37%), and H_2O_2 (30%) in a volumetric ratio of 10:1:1. The gold coverglass was then rinsed with copious amounts of water and used immediately for AFM measurements.

AFM Measurements. AFM measurements were conduced on a custom-built AFM operating with an Asylum Research MFP-3D controller. The spring constant of the polymer-modified cantilever was determined using the equipartition theorem, which provided an accuracy of ±10%. The spring constant for the lever used in this study was determined to be 14.72 pN/nm, with a deflection inverse optical lever sensitivity of 263 nm/V and resonant frequency of ~1.2 kHz in phosphate buffered saline (137 mM NaCl). After acquiring several thousand force−extension curves in phosphate buffer, the buffer was changed to a phosphate buffered saline containing 1 M NaCl to collapse the polymer, and the cantilever was recalibrated, yielding a spring constant of 12.37 pN/nm, with an inverse optical lever sensitivity of 279. The protocol to acquire force−extension traces was as follows: the AFM was programmed to approach the surface at 3000 nm/s until a trigger force of 250 pN was reached, indicating the tip had made contact with the surface. The dwell time for the tip at the surface was 0.5 s, after which the tip was retracted at 500, 1500, or 5000 nm/s for a total distance of 750 nm.

Conflict of Interest: The authors declare no competing financial interest.

Supporting Information Available: Size-exclusion chromatograms (Figure S1), proton NMR spectrum (Figure S2), additional cloud-point curves (Figure S3), WLC force−extension traces in low salt (Figure S4) and high salt (Figure S5) buffers, estimated WLC persistence length plot (Figure S6), and pulling speed dependency of plateau height (Figure S7). This material is available free of charge *via* the Internet at http://pubs.acs.org.

REFERENCES AND NOTES

1. Klee, D.; Hocker, H. Polymers for Biomedical Applications: Improvement of the Interface Compatibility. *Biomedical Applications: Polymer Blends*; Springer-Verlag: Berlin, 1999; Vol. 149, pp 1−57.
2. Kumar, A.; Srivastava, A.; Galaev, I. Y.; Mattiasson, B. Smart Polymers: Physical Forms and Bioengineering Applications. *Prog. Polym. Sci.* **2007**, *32*, 1205–1237.
3. Balazs, A. C.; Emrick, T.; Russell, T. P. Nanoparticle Polymer Composites: Where Two Small Worlds Meet. *Science* **2006**, *314*, 1107–1110.
4. Costa, R. R.; Custodio, C. A.; Arias, F. J.; Rodriguez-Cabello, J. C.; Mano, J. F. Layer-by-Layer Assembly of Chitosan and Recombinant Biopolymers into Biomimetic Coatings with Multiple Stimuli-Responsive Properties. *Small* **2011**, *7*, 2640–2649.
5. Lee, J.; Kim, O.; Jung, J.; Na, K.; Heo, P.; Hyun, J. Simple Fabrication of a Smart Microarray of Polystyrene Microbeads for Immunoassay. *Colloids Surf., B* **2009**, *72*, 173–180.
6. Pareek, P.; Adler, H. J. P.; Kuckling, D. Tuning the Swelling Behavior of Chemisorbed Thin PNIPAAM Hydrogel Layers by N,N-Dimethyl Acrylamide Content. In *Characterization of Polymer Surfaces and Thin Films*; Grundke, K., Stamm, M., Adler, H. J., Eds.; Springer-Verlag: Berlin, 2006; pp 145−151.
7. Friedsam, C.; Gaub, H. E.; Netz, R. R. Probing Surfaces with Single-Polymer Atomic Force Microscope Experiments. *Biointerphases* **2006**, *1*, MR1–MR21.
8. Staple, D. B.; Geisler, M.; Hugel, T.; Kreplak, L.; Kreuzer, H. J. Forced Desorption of Polymers from Interfaces. *New J. Phys.* **2011**, *13*.

9. Geisler, M.; Netz, R. R.; Hugel, T. Pulling a Single Polymer Molecule off a Substrate Reveals the Binding Thermodynamics of Cosolutes. *Angew. Chem., Int. Ed.* **2010**, *49*, 4730–4733.

10. Zhang, M. Q.; Desai, T.; Ferrari, M. Proteins and Cells on PEG Immobilized Silicon Surfaces. *Biomaterials* **1998**, *19*, 953–960.

11. Lutz, J. F. Polymerization of Oligo(ethylene glycol) (meth)-acrylates: Toward New Generations of Smart Biocompatible Materials. *J. Polym. Sci., Polym. Chem.* **2008**, *46*, 3459–3470.

12. Lutz, J. F.; Hoth, A. Preparation of Ideal PEG Analogues with a Tunable Thermosensitivity by Controlled Radical Copolymerization of 2-(2-Methoxyethoxy)ethyl Methacrylate and Oligo(ethylene glycol) Methacrylate. *Macromolecules* **2006**, *39*, 893–896.

13. Benmouna, F.; Johannsmann, D. Hydrodynamic Interaction of AFM Cantilevers with Solid Walls: An Investigation Based on AFM Noise Analysis. *Eur. Phys. J. E* **2002**, *9*, 435–441.

14. Lutz, J.-F. Thermo-Switchable Materials Prepared Using the OEGMA-Platform. *Adv. Mater.* **2011**, *23*, 2237–2243.

15. Becer, C. R.; Hahn, S.; Fijten, M. W. M.; Thijs, H. M. L.; Hoogenboom, R.; Schubert, U. S. Libraries of Methacrylic Acid and Oligo(ethylene glycol) Methacrylate Copolymers with LCST Behavior. *J. Polym. Sci., Part A: Polym. Chem.* **2008**, *46*, 7138–7147.

16. Lutz, J.-F.; Akdemir, O.; Hoth, A. Point by Point Comparison of Two Thermosensitive Polymers Exhibiting a Similar LCST: Is the Age of Poly(NIPAM) Over? *J. Am. Chem. Soc.* **2006**, *128*, 13046–13047.

17. Venkataraman, S.; Ong, W. L.; Ong, Z. Y.; Loo, S. C. J.; Ee, P. L. R.; Yang, Y. Y. The Role of PEG Architecture and Molecular Weight in the Gene Transfection Performance of PEGylated Poly(dimethylaminoethyl methacrylate) Based Cationic Polymers. *Biomaterials* **2011**, *32*, 2369–2378.

18. Giannotti, M. I.; Vancso, G. J. Interrogation of Single Synthetic Polymer Chains and Polysaccharides by AFM-Based Force Spectroscopy. *ChemPhysChem* **2007**, *8*, 2290–2307.

19. Sonnenberg, L.; Billon, L.; Gaub, H. E. Competitive Adhesion Reduces the Effective Bridging Length of Polymers. *Macromolecules* **2008**, *41*, 3688–3691.

20. Kufer, S. K.; Puchner, E. M.; Gumpp, H.; Liedl, T.; Gaub, H. E. Single-Molecule Cut-and-Paste Surface Assembly. *Science* **2008**, *319*, 594–596.

21. Kellermayer, M. S. S. Z.; Grama, L. S.; Karsai, A. D.; Nagy, A.; Kahn, A.; Datki, Z. L.; Penke, B. Reversible Mechanical Unzipping of Amyloid β-Fibrils. *J. Biol. Chem.* **2005**, *280*, 8464–8470.

22. Cho, Y.; Zhang, Y.; Christensen, T.; Sagle, L. B.; Chilkoti, A.; Cremer, P. S. Effects of Hofmeister Anions on the Phase Transition Temperature of Elastin-like Polypeptides. *J. Phys. Chem. B* **2008**, *112*, 13765–13771.

23. Friedsam, C.; Gaub, H. E.; Netz, R. R. Adsorption Energies of Single Charged Polymers. *Europhys. Lett.* **2007**, *72*, 844–850.

24. Geisler, M.; Balzer, B. N.; Hugel, T. Polymer Adhesion at the Solid−Liquid Interface Probed by a Single-Molecule Force Sensor. *Small* **2009**, *5*, 2864–2869.

25. Jones, D. M.; Smith, J. R.; Huck, W. T. S.; Alexander, C. Variable Adhesion of Micropatterned Thermoresponsive Polymer Brushes: AFM Investigations of Poly(N-isopropylacrylamide) Brushes Prepared by Surface-Initiated Polymerizations. *Adv. Mater.* **2002**, *14*, 1130–1134.

26. Valiaev, A.; Lim, D. W.; Schmidler, S.; Clark, R. L.; Chilkoti, A.; Zauscher, S. Hydration and Conformational Mechanics of Single, End-Tethered Elastin-like Polypeptides. *J. Am. Chem. Soc.* **2008**, *130*, 10939–10946.

27. Cecchet, F.; Lussis, P.; Jérôme, C.; Gabriel, S.; Silva-Goncalves, E.; Jérôme, R.; Duwez, A.-S. A Generic Chemical Platform for Molecular Recognition and Stimuli-Responsive Probes Based on Scanning Probe Microscopy. *Small* **2008**, *4*, 1101–1104.

28. Fustin, C. A.; Duwez, A. S. Dithioesters and Trithiocarbonates Monolayers on Gold. *J. Electron Spectrosc. Relat. Phenom.* **2009**, *172*, 104–106.

29. Puchner, E. M.; Franzen, G.; Gautel, M.; Gaub, H. E. Comparing Proteins by Their Unfolding Pattern. *Biophys. J.* **2008**, *95*, 426–434.

30. Alcaraz, J.; Buscemi, L.; Puig-De-Morales, M.; Colchero, J.; Baro, A.; Navajas, D. Correction of Microrheological Measurements of Soft Samples with Atomic Force Microscopy for the Hydrodynamic Drag on the Cantilever. *Langmuir* **2002**, *18*, 716–721.

31. Kestin, J.; Khalifa, H. E.; Correia, R. J. Tables of the Dynamic and Kinematic Viscosity of Aqueous NaCl Solutions in the Temperature Range 20−150 °C and the Pressure Range 0.1−35 MPa. *J. Phys. Chem. Ref. Data* **1981**, *10*, 71–88.

ARTICLE